

DEC 23 1946

ACR No. L4B28

NATIONAL ADVISORY COMMITTEE FOR AERONAUTICS

WARTIME REPORT

ORIGINALLY ISSUED

February 1944 as
Advance Confidential Report L4B28

CONSIDERATIONS OF WAKE-EXCITED VIBRATORY STRESS

IN A PUSHER PROPELLER

By Blake W. Corson, Jr., and Mason F. Miller

Langley Memorial Aeronautical Laboratory
Langley Field, Va.

NACA

WASHINGTON

NACA LIBRARY
LANGLEY MEMORIAL AERONAUTICAL
LABORATORY
Langley Field, Va.

NACA WARTIME REPORTS are reprints of papers originally issued to provide rapid distribution of advance research results to an authorized group requiring them for the war effort. They were previously held under a security status but are now unclassified. Some of these reports were not technically edited. All have been reproduced without change in order to expedite general distribution.

NATIONAL ADVISORY COMMITTEE FOR AERONAUTICS

ADVANCE CONFIDENTIAL REPORT NO. L4B28

CONSIDERATIONS OF WAKE-EXCITED VIBRATORY STRESS

IN A PUSHER PROPELLER

By Blake W. Corson, Jr., and Mason F. Miller

SUMMARY

An equation based on simple blade-element theory and the assumption of a fixed wake pattern is derived and fitted to available data to show the first-order relation between the parameters of propeller operation and the intensity of the wake-excited periodic force acting on the blades of a pusher propeller. The derived equation indicates that the intensity of the wake-excited periodic force is directly proportional to air density, to airspeed, to rotational speed, and to propeller-disk area.

The derived equation indicates that the effect of power coefficient upon the intensity of the wake-excited periodic force is small. In normal operation the vibratory force decreases with increasing power coefficient. If a pusher propeller is used as a brake, increasing the power coefficient will increase the vibratory force.

For geometrically similar pusher propellers, a propeller of large diameter will, in general, experience less wake-excited vibratory stress than a propeller of smaller diameter.

Limited experimental data indicate that the wake-excited vibratory stress in a propeller increases with the drag of the body producing the wake.

INTRODUCTION

With the increased consideration being given to the use of pusher propellers there has arisen a concern over the magnitude of the periodic stresses peculiar to this type of propeller. A pusher propeller usually operates in the wake of some other part of the airplane, such as the wing, engine mount, or tail surface. As the

propeller rotates, each blade passes alternately from a region where the slipstream axial velocity is practically the same as the velocity of the free air stream into the wake region, where the axial velocity may be considerably reduced. When a blade passes through the wake, the blade sections experience an increase in angle of attack and a slight decrease in dynamic pressure; the aerodynamic load on the blade thus changes periodically. The type of motion with which the propeller will vibrate may depend upon several factors, two of which are the number of blades and the location of the propeller relative to the wake. The response as measured by the stress produced in a blade depends upon the deflection shape of the blade as well as upon the intensity of the exciting force.

The vibratory stress in a four-blade single-rotating propeller operating in the wake of a wing has been measured in the LMAL 16-foot high-speed tunnel and the results of the tests have been reported in reference 1. In that report no detailed study was made of the influence of the aerodynamic conditions of operation upon the propeller vibratory stress.

The purpose of the present report is to derive a simple expression that will show the first-order effects of airspeed, rotational speed, propeller characteristics, propeller size, and wake size upon the periodic force which excites vibrations in a propeller operating in the wake of a wing. If an attempt is made to account for all obvious effects of the propeller and wake upon each other, the problem becomes involved if not unmanageable. In order to maintain simplicity of the final expression, it was necessary to make several assumptions, which will be discussed herein.

ASSUMPTIONS

The problem of estimating the variation of the periodic aerodynamic load on the blade of a propeller operating in a wake is limited here, first, to a particular type of propeller installation and, second, to operating conditions for which the induced velocities are negligibly small. The installation being considered is a pusher propeller located behind a wing with the axis of rotation centered in the profile of the wake

of the wing. It is assumed that the propeller disk is large enough to extend beyond the wing wake into the undisturbed air stream. The wing drag coefficient is assumed to be constant with airspeed; this assumption implies a fixed wake pattern with the result that at a given point in the wake the velocity defect will always be proportional to the airspeed. A diagram showing a typical distribution of velocity in the wake of a wing is presented in figure 1. (See reference 2.)

In order to estimate the first-order periodic change of the aerodynamic load on a propeller blade due to intermittent change in axial velocity, simple blade-element theory (reference 3) is assumed to be adequate. The effect of the changes in axial velocity upon the blade-section drag characteristics is regarded as negligible. Blade-section lift, therefore, is the only force considered in the blade-element analysis.

For all conditions under which the propeller blade sections exert lift, they maintain a consequent induced air flow having both axial and rotational velocity components at the propeller. At speeds above the take-off and climb range the induced axial velocity is very small in comparison with the forward speed. For a steady condition of normal operation the velocities induced at various stations along the propeller blade can be estimated by the procedure given in reference 4. This procedure, however, cannot be applied at present because the propeller operates with unsteady lift. When the rotating propeller blade traverses the wake, the blade sections exert a greater lift, which creates an increase in the induced velocity. The instantaneous change in lift exerted by the propeller blade sections during their passage through the wake is less than is to be expected from the corresponding change in angle of attack, because development of the circulation in unsteady lift lags behind the angle-of-attack change (reference 5). A comprehensive treatment of the problem would require such specific assumptions concerning the shape of the wake and the distribution and magnitude of the velocity induced at the propeller that any solution obtained would be neither simple nor general. The straightforward approach permitted by the use of simple blade-element theory and the assumption of a fixed wake pattern justifies the consequent slight loss of accuracy.

SYMBOLS

V	airspeed and slipstream axial velocity at propeller disk, feet per second or miles per hour (assumed identical in this analysis)
V _R	resultant velocity of air relative to any blade element, feet per second
n	propeller rotational speed, revolutions per second
D	diameter of propeller, feet
J	advance ratio (V/nD)
R	propeller tip radius, feet
r	radius to any blade element, feet
x	fraction of tip radius (r/R)
b	chord of any blade element, feet
θ	blade angle of any blade element measured from zero-lift direction, radians
φ	effective helix angle for any blade element, radians $\left(\tan^{-1} \frac{V}{2\pi rn}\right)$
α	angle of attack of any blade element, radians (θ - φ)
α _w	angle of attack of wing
L	lift, pounds
L _c	coefficient of differential lift $\left(\frac{\frac{dL}{dx}}{\rho n^2 D^4}\right)$
C _L	lift coefficient
$\overline{C_L}$	mean lift coefficient, effective over entire blade
$m = \frac{dC_L}{d\alpha}$	= 5.7 (approx.)

T	thrust (propeller-shaft tension), pounds
Q	torque, foot-pounds
P	power, foot-pounds per second
ρ	density of air, slugs per cubic foot
C_T	thrust coefficient ($T/\rho n^2 D^4$)
C_P	power coefficient ($P/\rho n^3 D^5$)
η	propeller efficiency
B	number of blades of a single propeller
C_1, C_2, C_3	constants
Subscript:	
0.7R	at 0.7R

DERIVATION OF EQUATION FOR EXCITING FORCE

For a propeller operating in the wake of an airfoil at thrust-axis level a relation between vibratory exciting force and the parameters of propeller operation can be derived by first expressing the force on a propeller blade element. The lift force on a propeller blade element of differential radial length (fig. 2) is

$$dL = \frac{1}{2} \rho V_R^2 b C_L dr \quad (1)$$

If the coefficient of differential lift is defined as

$$L_c = \frac{\frac{dL}{dr}}{\rho n^2 D^4} \quad (2)$$

equation (1) can be put into the form

$$L_c = \frac{\pi^2}{4} \frac{b}{D^2} C_L \sec^2 \phi$$

UNCLASSIFIED

6

NACA ACR No. L4B28

The change in coefficient of differential lift caused by a differential change in forward velocity is

$$\frac{dL_c}{dV} = \frac{\pi^2 b x^2}{4D} \left(\sec^2 \phi \frac{dC_L}{dV} + C_L \frac{d}{dV} \sec^2 \phi \right) \quad (3)$$

The lift coefficient may be expressed as the product of the lift-curve slope and the difference between blade angle and helix angle; that is,

$$\begin{aligned} C_L &= m\alpha \\ &= m(\beta - \phi) \end{aligned}$$

If the blade angle is assumed not to change with rapid changes in axial velocity,

$$\frac{dC_L}{dV} = -m \frac{d\phi}{dV} \quad (4)$$

By performing the operations of equation (3) and using equation (4), there is obtained

$$\frac{dL_c}{dV} = \frac{\pi^2 b x^2}{4D} \left[-m \sec^2 \phi \frac{d\phi}{dV} + C_L \left(2 \sec^2 \phi \tan \phi \frac{d\phi}{dV} \right) \right] \quad (5)$$

By figure 2,

$$\tan \phi = \frac{V}{\pi x n D}$$

from which

$$\sec^2 \phi \frac{d\phi}{dV} = \frac{1}{\pi x n D}$$

These relations when substituted in equation (5) yield

$$\frac{dL_c}{dV} = \frac{b}{4\pi^2 D^3} (2VC_L - m\pi x n D)$$

UNCLASSIFIED

which, from equation (2), gives

$$d\left(\frac{dL}{dV}\right) = \frac{\rho D^2}{4} \left(2VC_L \frac{b}{D} dx - \pi m D x \frac{b}{D} dx \right) \quad (6)$$

The integration of equation (6) gives the following relation between the change in lift on the entire propeller blade and the change in axial velocity:

$$dL = \frac{\rho D^2}{4} \left(2V \int_{0.2}^{1.0} C_L \frac{b}{D} dx - \pi m D \int_{0.2}^{1.0} x \frac{b}{D} dx \right) dV \quad (7)$$

Examination of equation (7) shows that, of the terms within brackets, the one containing C_L will, in general, be small in comparison with the other. An explicit relation between C_L and x does not exist, but equation (7) can be simplified with small loss of accuracy by using a mean value of lift coefficient $\overline{C_L}$ regarded as effective and constant along the blade. In reference 6 Lock shows that the thrust coefficient of a propeller can be computed with fair accuracy from an elemental thrust coefficient, at $x = 0.7$, by using the integrating factor $\pi/4$. A derivation based on the use of this factor is given in the appendix, which shows an approximate relation between the effective lift coefficient and the propeller operating characteristics.

$$\begin{aligned} \overline{C_L} &= C_{L0.7R} \\ &= \frac{32}{\pi^2 B \left(\frac{b}{D}\right)_{0.7R}} \frac{C_T}{\sqrt{J^2 + 4.84}} \end{aligned} \quad (8)$$

When a mean value of lift coefficient is used, two integrals that depend only on the geometry of the propeller blade remain in equation (7). For a given blade design these integrals are constants and may be evaluated graphically from the relations

UNCLASSIFIED

8

NACA ACR No. L4B28

$$C_1 = \int_{0.2}^{1.0} \frac{b}{D} dx$$

$$C_2 = \int_{0.2}^{1.0} \frac{b}{D} x dx$$

When the constants C_1 and C_2 and the expression for mean lift coefficient (equation (8)) are substituted in equation (7), there results

$$dL = \frac{\rho n D^3}{4} \left[\frac{64}{\pi^2 B} \frac{C_1}{\left(\frac{b}{D}\right)_{0.7R}} \frac{C_T J}{\sqrt{J^2 + 4.84}} - \pi C_2 \right] dV$$

The assumption of a fixed wake pattern permits the concept that the velocity defect at a given point in the wake is always proportional to the airspeed; thus

$$\Delta V = -C_3 V \quad (9)$$

This definition is used herein without regard to the ratio of blade width to wake thickness. Further consideration of the effect of wake size upon the vibratory exciting force is given under "Discussion." By regarding dL and dV as finite increments and using equation (9), the intensity of the propeller-blade vibratory exciting force is expressed as

$$\Delta L = C_3 \frac{\rho n D^3}{4} \left[\pi C_2 - \frac{64}{\pi^2 B} \frac{C_1}{\left(\frac{b}{D}\right)_{0.7R}} \frac{C_T J}{\sqrt{J^2 + 4.84}} \right] V \quad (10)$$

The substitution of an average lift coefficient (equation (8)) in equation (7) provides a means of expressing the steady operating condition of the propeller in terms of customary parameters. The effect of distribution of lift increment along the blade upon the

UNCLASSIFIED

wake-excited propeller vibration depends upon the blade-deflection shape. For a given type of blade deflection the vibratory force should be governed by equation (10).

DISCUSSION

General.-- The expression for the magnitude of the vibratory exciting force (equation (10)) shows the relation between aerodynamic exciting force and dimensions. If the quantities in the brackets are disregarded, the force is proportional to air density ρ , to an area D^2 , and to the square of velocity having the components rotational speed nD and airspeed V . Of the terms within the brackets, $m\pi C_2$ determines the greater part of the exciting force that is due to the increased angle of attack of the blade sections within the wake. The term that includes C_{TJ} represents the change in force due to the decreased dynamic pressure within the wake (equation (3)). Actually the term involving C_{TJ} (equal to $C_p\eta$) is relatively small and minimizes the effect of $m\pi C_2$ in the range of normal operation. Retention of the term C_{TJ} is desirable, however, because, if the propeller is used as a brake, the thrust coefficient becomes negative and the effects of the quantities within the brackets are additive; the result is that, other conditions being equal, greater vibratory forces are experienced.

Effect of wake size.-- In deriving equation (10) no effort was made to account for the effect of variation of propeller location downstream from the trailing edge of the wing nor of the wake thickness. The assumption of a fixed wake pattern permitted the statement that the ratio of wake-velocity defect to airspeed is constant (equation (9)). It is known that the wake pattern (velocity profile) in a given wing wake changes with distance downstream from the wing (reference 2). Close behind the wing the wake is thin and the velocity defect is intense; farther downstream the wake is thicker and the velocity defect is reduced. Both wake profiles represent the same momentum loss, and the velocity defect integrated across the wake is approximately the same at all stations within a distance of several wing chords behind the wing. As the downstream location of

the propeller is changed, the time required for a blade section to traverse the wake changes in inverse proportion to the velocity defect and therefore inversely as the exciting-force intensity. The vibratory exciting impulse, which is the product of force and time, remains constant. Although vibratory stress in the wing structure may be considerably affected by downstream location of the propeller, it is probable that the wake-excited vibratory stress in the propeller is very little affected.

No data are available that show directly the effect of wake size but the vibratory stress in the propeller blade shank measured at constant airspeed, rotational speed, and power varied directly with estimated wing drag with and without flap (reference 1). These limited data, as well as dimensional analysis, indicate that the constant C_3 and therefore wake-excited vibratory stress in a pusher propeller are proportional to the profile drag of the wing producing the wake.

Effect of propeller diameter.- In general, pusher propellers of large diameter will experience less wake-excited vibratory stress than propellers of small diameter. Consider the following cases:

Case 1. Two pusher-propeller installations of different size but geometrically similar with respect to propeller, wing, and wake dimensions operate at the same airspeed and with the same rotational tip speed. Equation (10) indicates an exciting load proportional to D^2 . If a blade is regarded as a beam, the unit bending load increases directly with D and the bending moment at a given station therefore increases as D^2 . The section modulus at any station also increases as D^3 . The wake-excited stress would therefore be the same for both propellers for a given mode of vibration if the two resonant conditions occurred at the same rotational tip speed. Because the propeller rotational speed is inversely proportional to D , as is also the static vibration frequency for a given mode, the resonant condition for the two propellers would occur at the same rotational tip speed if the vibratory frequency did not change with rotational speed. When the effect of centrifugal force on the resonant frequency of the blade is considered (reference 7), it is seen that resonance will occur for the propeller of large diameter at a lower rotational tip speed than for the smaller propeller and therefore, by equation (10), the vibratory stress will be less.

Case 2. On a given airplane a change is made from a pusher propeller of small diameter to a similar propeller of larger diameter. The rotational tip speed and airspeed are the same for both propellers. This case is identical with case 1 except that the ratio of wake area to slipstream cross-sectional area at the propeller disk is reduced. For this reason as well as for the reason given in case 1 the vibratory exciting force and consequently the stress will be less for a pusher propeller of large diameter than for a small propeller.

Compressibility effect.- The compressibility of air affects the propeller vibratory exciting force only to the extent that it affects the blade-section airfoil characteristics and the wing wake. The quantity m within the brackets of equation (10) increases with blade-section operating Mach number and produces a corresponding increase in the thrust coefficient C_T . The net effect is an increase in exciting force due to compressibility with an increase in either rotational tip speed or airspeed. This increase in exciting force is in addition to the direct effect of the rotational tip speed or airspeed indicated by equation (10). In general, airplanes do not operate at such high airspeeds that wing drag (wake size) is much affected by compressibility; however in some cases propeller vibratory stress may be influenced by the effect of compressibility on the wing drag. Airplanes having wing sections with a thickness ratio of 20 to 23 percent may operate at high altitude at a value of Mach number close to the critical value (0.5 to 0.6) for the wing. It would be possible in a shallow dive to exceed the critical Mach number and thereby to increase the wing drag and in turn the propeller vibratory stress.

Excitation frequency.- In turning through one revolution, each blade of a pusher propeller operating in the wake of a wing located at thrust-axis level receives two wake-excited impulses. Any mode of propeller vibration having a resonant frequency of $2n$ may be excited by the wake. Because the wake region through which the propeller operates may be quite sharply defined, the excitation will contain harmonics of the frequency $2n$. The harmonic components, however, are of relatively small importance according to the tests of references 1 and 8. Although previous tests (reference 9) indicate that it is possible to produce a second mode of vibration with aerodynamic excitation, the first modes of

vibration occur most frequently with such excitation (references 1, 8, and 9); therefore primary interest is in the vibrations that have a frequency of $2n$.

APPLICATION OF EXCITING-FORCE EQUATION TO MEASURED DATA

Apparatus and methods.- During the tests reported in reference 1 the propeller operated behind a wing mounted at thrust-axis level (fig. 3). The plane of the propeller disk was located about 23 percent of the wing chord behind the trailing edge, or approximately 2 blade chords (at the 0.75R) behind the wing trailing edge. The wing was tapered and had NACA low-drag sections. A simulated full-span split flap was attached to the wing for some of the tests. The propeller was driven by a Pratt & Whitney R-2300 engine mounted in a nacelle and supported in the wind tunnel separately from the wing. The single-rotating propeller was a Hamilton Standard hydromatic of 12-foot diameter, which had four aluminum-alloy blades of design 6487-12 used in a hub of design 24D50. The propeller rotated at nine-sixteenths of the engine speed.

The experimental data consisted in oscillograph and wave-analyzer records of strain, which were converted to stress; electrical strain gages were used for pickups. The stress determinations are believed to be accurate to within ± 5 percent. The method and accuracy of strain recordings are explained in more detail in reference 9. The strain-gage circuits were completed through a commutator in front of the propeller. Leads from the commutator were supported by a steel cable $3/8$ inch in diameter stretched across the wind tunnel just behind the wing. The propeller operated in the combined wake of the wing and the cable.

Tests and results.- The propeller-blade vibratory stress was measured during tests in which the rotational speed was held constant at the resonant speed and in which engine torque, and therefore power coefficient, was held constant. Only the airspeed was varied during a run. Three runs were made with different constant values of power coefficient. An edgewise reactionless vibration was encountered, which produced maximum stresses near the blade shank.

If damping is assumed to be constant, the vibratory stress for a given propeller is proportional to the exciting force ΔL for any given resonant frequency. In a strict sense, the damping changes when ΔL changes; for example, a change in airspeed V would be accompanied by changes in aerodynamic damping and mechanical hysteresis damping. In the application of equation (10) to the available test data, however, it is assumed that, within the accuracy of the equation and of the vibratory-stress measurements, the change in the damping is small. For constant damping, the propeller vibratory stress under the conditions of the tests should have increased directly as the airspeed increased. A slight effect of power coefficient might have been expected but, because $C_{p\eta}$ is practically constant in the operating range, this effect would be very small. The results of the stress measurements are given in table I and are shown graphically in figure 4, in which vibratory stress at the propeller blade shank is plotted against airspeed. The straight-line variation of stress with airspeed required by equation (10) has been fitted to the data from reference 1 by the method of least squares, and the agreement is reasonably good. There was no consistent variation of vibratory stress with power coefficient.

A few additional measurements of propeller-blade vibratory stress were made after a simulated split flap was attached to the wing ahead of the propeller. The deflected flap caused such a great increase in the vibratory stress that, when the airspeed was increased above 150 miles per hour, the vibratory stress became dangerous. The stress increase produced by the deflected flap is attributed solely to the increase in wing drag and not to the downwash associated with the change in wing lift; this conclusion is based upon the test results of reference 1, which show that increasing the angle of attack of the wing from 0° to 3.9° produced practically no increase of vibratory stress at a frequency of $2n$. There are available only two sets of test data by which wake-excited vibratory stress may be correlated with the drag of the body producing the wake. These data taken from reference 1 are presented in figure 5, which shows vibratory stress of frequency $2n$ measured at the blade shank. The drag coefficient based on wing area was computed from the combined estimated drag of the wing and electrical-lead support cable.

CONCLUSIONS

The derived equation that shows the first-order relation between the intensity of the wake-excited periodic force acting on a propeller blade and the parameters of propeller operation and limited experimental data indicate the following conclusions:

1. The intensity of the wake-excited periodic force acting on the blade of a propeller operating in the wake of a wing varies directly with air density, airspeed, rotational speed, and propeller-disk area.

2. The magnitude of the power coefficient has a very small effect upon the magnitude of the wake-excited periodic force that causes vibration in a pusher propeller. In normal operation, increasing the power coefficient decreases the vibratory force. When the propeller is used as a brake, increasing the power coefficient intensifies the periodic force.

3. For geometrically similar propellers, a pusher propeller of large diameter will, in general, experience less wake-excited vibratory stress than one of smaller diameter.

4. The wake-excited vibratory stress in a propeller increases with the drag of the body producing the wake.

APPENDIX

DERIVATION OF EXPRESSION FOR EFFECTIVE LIFT COEFFICIENT

Refer to figure 2.

$$dT = B dL \cos \phi$$

$$dL = \frac{1}{2} \rho [V^2 + (2\pi r n)^2] C_L b dr$$

$$\cos \phi = \frac{2\pi r n}{\sqrt{V^2 + (2\pi r n)^2}}$$

$$= \frac{\pi x}{\sqrt{J^2 + (\pi x)^2}}$$

$$dT = \frac{\rho \pi x [V^2 + (2\pi r n)^2] B C_L b}{2 \sqrt{J^2 + (\pi x)^2}} dr$$

$$dT = \frac{\rho n^2 D^4 [J^2 + (\pi x)^2] C_L \frac{b}{D} \pi x}{4 \sqrt{J^2 + (\pi x)^2}} dx$$

$$\frac{dT}{2\rho n^2 D^4 x dx} = \frac{dC_T}{d(x^2)}$$

$$= \frac{\pi \sqrt{J^2 + (\pi x)^2}}{8} B \frac{b}{D} C_L$$

By regarding the operation of propeller sections at $x = 0.7$ as representative of average operation of sections at all radii, Lock in reference 6 makes the approximation

$$C_T = \frac{\pi}{4} \left[\frac{dC_T}{d(x^2)} \right]_{0.7R}$$

which is also made here for convenience.

$$C_T = \frac{\pi^2}{32} \sqrt{J^2 + 4.84} B\left(\frac{b}{D}\right)_{0.7R} C_{L0.7R}$$

$$\overline{C_L} = C_{L0.7R}$$

$$= \frac{32}{\pi^2 B\left(\frac{b}{D}\right)_{0.7R}} \frac{C_T}{\sqrt{J^2 + 4.84}} \quad (8)$$

REFERENCES

1. Miller, Mason F.: Wind-Tunnel Vibration Tests of a Four-Blade Single-Rotating Pusher Propeller. ARR No. 3F24, NACA, June 1943.
2. Goett, Harry J.: Experimental Investigation of the Momentum Method for Determining Profile Drag. Rep. No. 660, NACA, 1939.
3. Weick, Fred E.: Aircraft Propeller Design. McGraw-Hill Book Co., Inc., 1930.
4. Lock, C. N. H., and Yeatman, D.: Tables for Use in an Improved Method of Airscrew Strip Theory Calculation. R. & M. No. 1674, British A.R.C., 1935.
5. Silverstein, Abe, and Joyner, Upshur T.: Experimental Verification of the Theory of Oscillating Airfoils. Rep. No. 673, NACA, 1939.
6. Lock, C. N. H.: A Graphical Method of Calculating the Performance of an Airscrew. R. & M. No. 1849, British A.R.C., 1938.
7. Den Hartog, J. P.: Mechanical Vibrations. McGraw-Hill Book Co., Inc., 2d ed., 1940.
8. Forshaw, J. R., Squire, H. B., and Bigg, F. J.: Vibration of Propellers Due to Non-Uniform Inflow. Rep. No. E.3938, R.A.E., April 1942.
9. Miller, Mason F.: Wind-Tunnel Vibration Tests of Dual-Rotating Propellers. ARR No. 5I11, NACA, Sept. 1943.

TABLE I
VIBRATORY STRESS AT SHANK FOR FIRST
MODE OF EDGEWISE VIBRATION

[Blade design, Hamilton Standard 6487-12; aluminum-alloy blades; no simulated split flap attached to wing; α_w , 0°]

Airspeed (mph)	Vibratory stress (lb/sq in.)
Power coefficient, 0.048	
106	± 2800
185	± 5650
280	± 7050
Power coefficient, 0.072	
142	± 3400
185	± 5500
280	± 6800
Power coefficient, 0.096	
157	± 4100
185	± 5600
280	± 6700

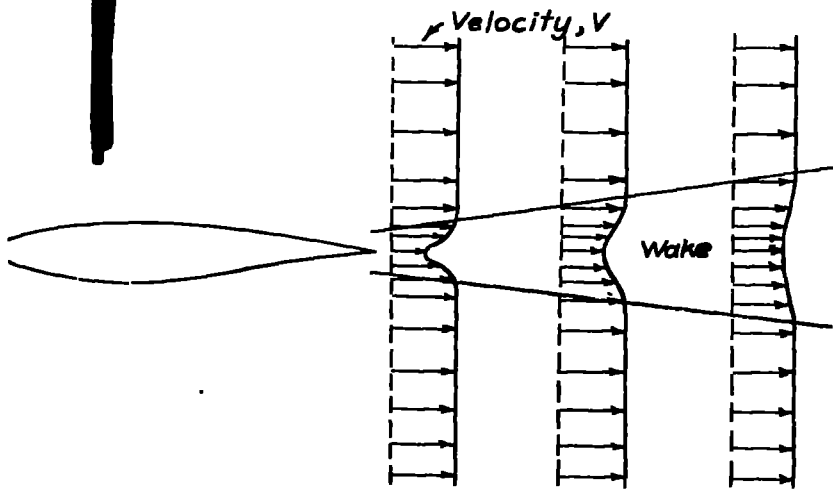


Figure 1.- A typical distribution of velocity in the wake of an airfoil.

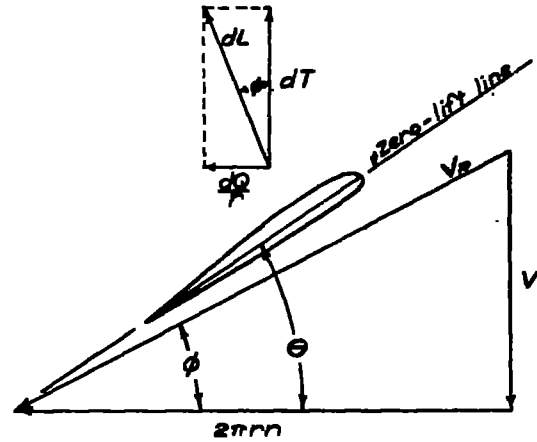


Figure 2.- Diagram of velocities and forces acting upon a blade element of differential radial length.

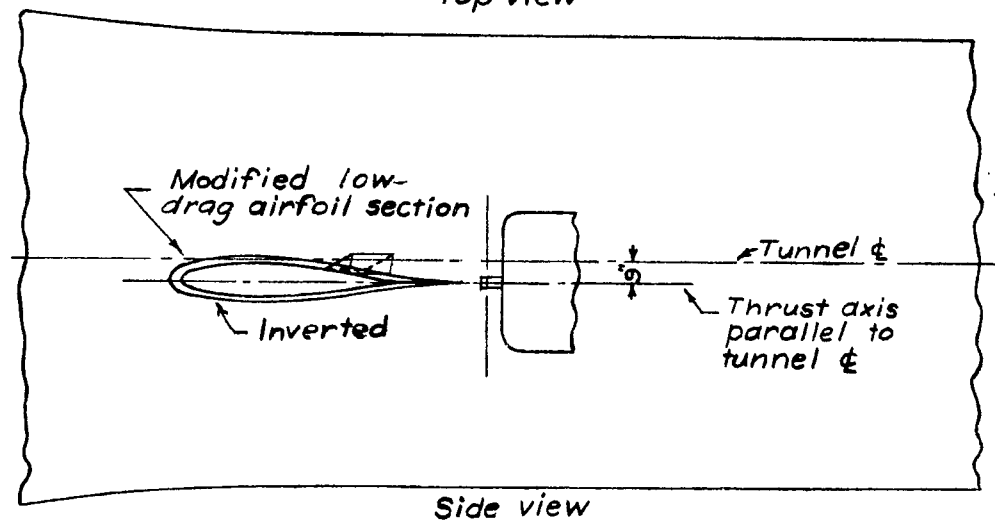
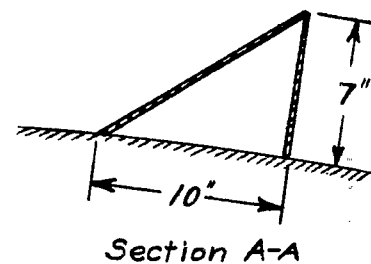
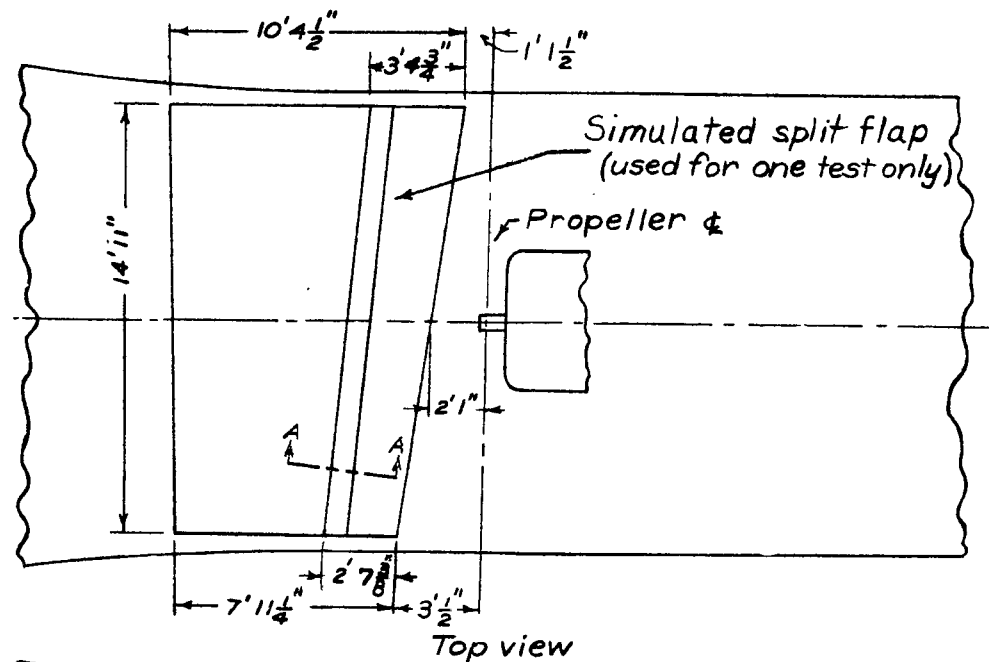


Figure 3.- Simulated pusher installation with simulated split flap attached to wing. $\alpha_w, 0^\circ$. (Fig. 2 of reference 1.)

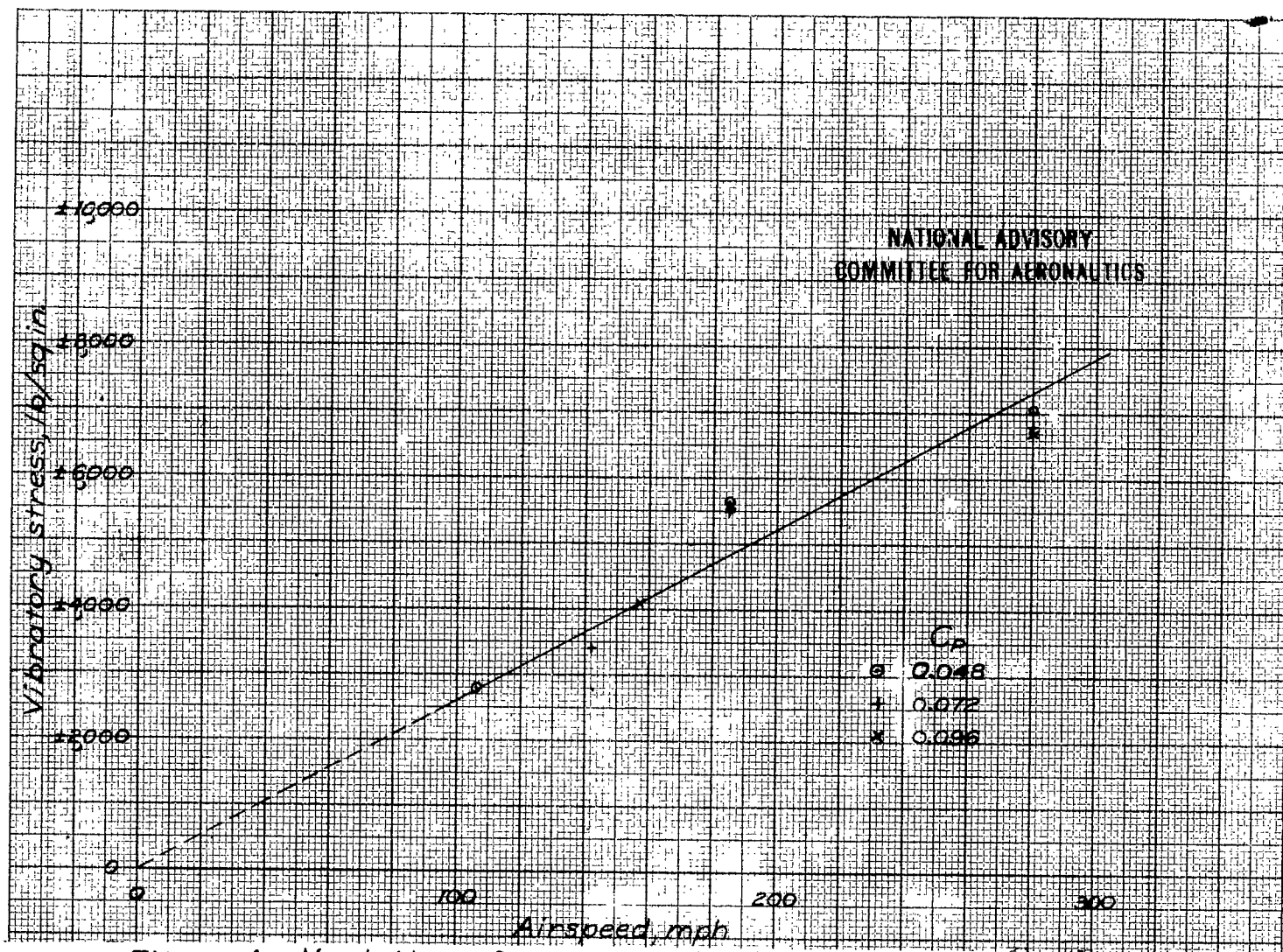
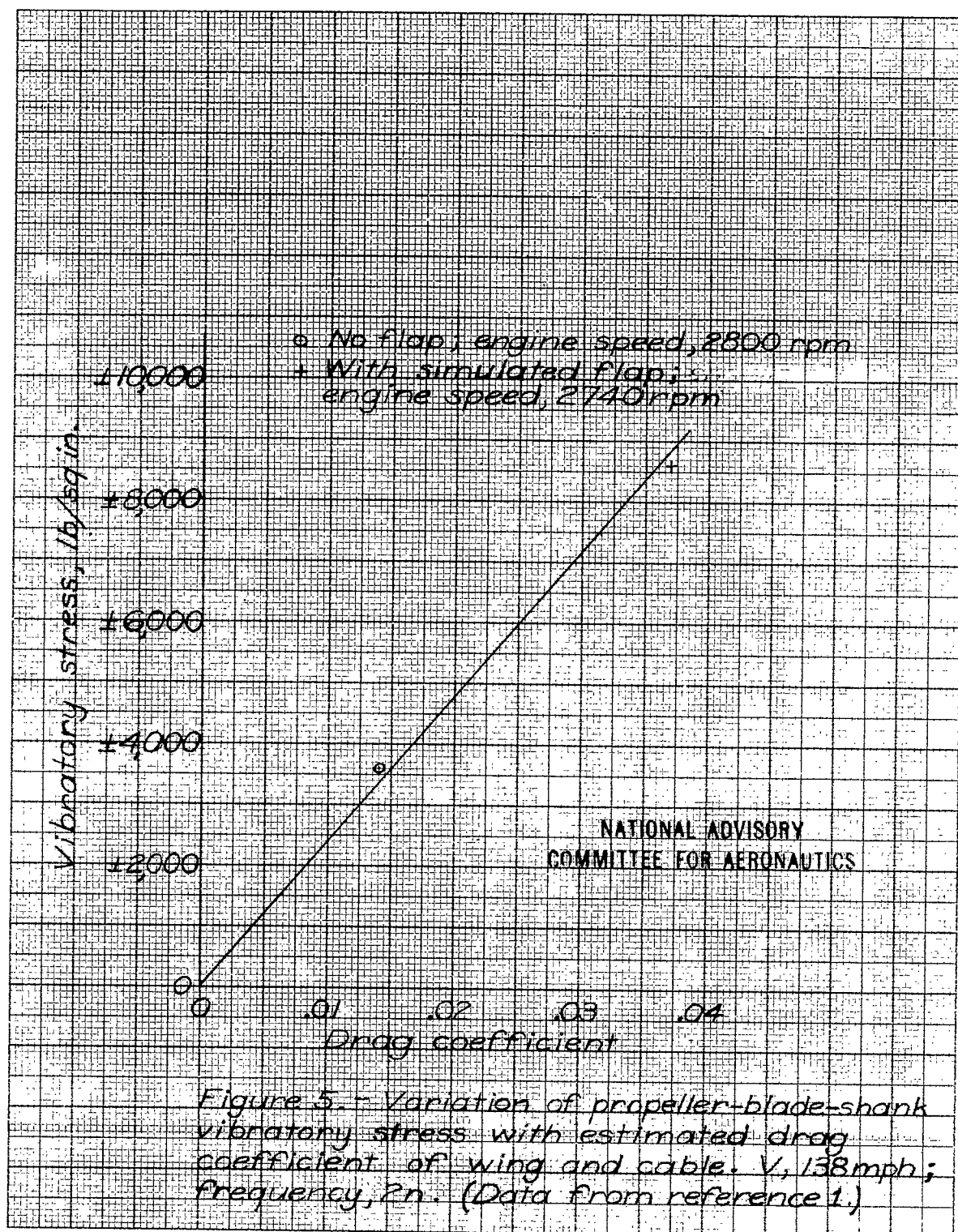


Figure 4. - Variation of propeller-blade-shank vibratory stress with airspeed. $\alpha_w, 0^\circ$; no flap on wing; frequency, $2n$; engine speed, 2800 rpm. (Data from reference 1.)





3 1176 01363 9019